An Effective Dental Work Extraction and Matching Method for Bitewing Radiographs

Chun-Hung Kuo
Computer Science and Information Engineering
Providence University
Shalu, Taichung 43301, Taiwan
g9872005@pu.edu.tw

Phen-Lan Lin*
Computer Science and Information Engineering
Providence University
Shalu, Taichung 43301, Taiwan
lan@pu.edu.tw

***Abstract*—This paper presents a method of dental work (DW) extraction and matching for bitewing radiographs. The method includes an algorithm that can correctly extract DW's from radiograph images and two matching metrics (d_{FD} of frequency domain and d_{XOR} of spatial domain) that can effectively match a postmortem DW to the genuine antemortem DW in the database. The experimental results show that our method can extract DW's more correctly shape- and number-wise than methods that use global thresholding. The results also show that, for a database containing 52 different shaped DW's, the accuracy based on d_{FD} is 95% when using top 6% retrievals and achieves to 100% when using top 17% retrievals; whereas the accuracy based on d_{XOR} is 86 and 95 %, respectively, when using the same percentage retrievals. For a database containing 10% of hoax DW's (i.e., DW's have the same shape but different orientation/position as some genuine DW's), the accuracy based on both metrics maintains about the same except the top-1 match based on d_{FD}. The fact that d_{XOR} was not affected by hoax DW's indicates that d_{FD} and d_{XOR} can compensate each other when matching the postmortem DW with hoax DW's. Comparing with the 95% and 100% hit rates using top 8% and 47% retrievals from a much bigger database reported in literature, the metric d_{FD} not only is more efficient but gives a better result.**

Keywords- Dental work extraction, Dental work matching, Bitewing radiograph, PM identification

I. INTRODUCTION

Biometric recognition systems based on characteristics such as finger print, face, voice, and iris can provide reliable human identification in many applications. However, most of these characteristics are not suitable for postmortem (PM) identification when the victims are under severe decaying of soft tissues or mass disasters such as fire or collision. Teeth, being the hardest and the most impregnable part of human body, are thus regarded as the best candidates for PM identification [1].

Many methods of human identification based on dental radiographs had been reported in literature [2]-[5].They mainly used teeth contours as the matching feature. Chen and Jain [3] proposed using dental works (DW's) as another feature in their method to improve its identification accuracy. Fig. 1 shows dental radiographs having DW's such as filling, crown, and bridge. As shown, most DW's appear brighter than teeth in dental radiographs and their contours are usually not as noisy as tooth contours, although the shapes are sometimes irregular. Thus, DW's can be used as an alternative or an additive feature besides tooth contour when performing human identification based on dental radiographs.

As the scale, the orientation, and the translation of PM radiographs and antemortem (AM) radiographs are generally different, each tooth must be firstly segmented and the query PM tooth must be aligned against the AM tooth under matching in preprocess when using spatial domain features, such as the size of the misaligned regions of DW's used in [3]. Many methods for teeth segmentation [1],[2] and alignment [3]-[6] have been proposed; nevertheless, imperfect alignment still occurs in cases such as unreliable or incomplete tooth contours due to poor image quality or images taken in rather different angles. Thus, using spatial domain features may encounter incorrect matching when any imposter DW happens to be similar to the genuine one in shape, position, and size, if the query tooth aligns better against the imposter tooth than the genuine tooth.

In this paper, we present a method of dental work extraction and matching for bitewing radiographs. Our method includes an algorithm that can correctly extract DW's from radiograph images and two matching metrics (d_{FD} of frequency domain and d_{XOR} of spatial domain) that can effectively match a postmortem DW to the genuine antemortem DW in the database. We extract DW's in two stages. In the first stage, we preprocess the image to reduce most irrelevant information of DW's before thresholding. We then filter the thresholded result to eliminate the remaining DW-irrelevant edge pixels to obtain the coarse contours of all DW's within the image. Finally the complete

*Corresponding Author

filling crown bridge

Figure 1. Dental radiographs with various types of dental works.

shape of each DW is obtained by region growing in stage 2. For the matching metrics, we define d_{xor} as the relative size of the misaligned region between the DW_{PM} and the DW_{AM} against which the DW_{PM} is affine transformed with the optimum parameters obtained from the best tooth contour matching, and d_{FD} as the root mean square error between the sets of Fourier descriptors representing the contour of each DW.

II. DENTAL WORK (DW) EXTRACTION

Same as the method in [7], our method also extracts DW's in two stages. But, instead of thresholding the entire image to get the coarse shapes of DW's in the first stage, we preprocess the image to reduce most irrelevant information of DW's before thresholding. We then filter the thresholded result to eliminate the remaining DW-irrelevant edge pixels to obtain the coarse contours of all DW's within the image. In Stage 2, we obtain the complete shape of each DW by region growing instead of by using a separate snake. A detailed description of our DW extraction method is as follows.

A. Extraction algorithm

Stage 1: Locate the coarse contours of all DW's within an image.

Step 1) Preprocess: Reduce DW-irrelevant pixels by Canny filter. As DW's appear brighter than teeth, we apply Canny edge filter [8],[9] to obtain the edge pixels around DW's. Because these resulted edges are not always step edges, the intensity of the DW edge pixels may not be as high as most DW pixels. Thus, we refine the edges by replacing each edge pixel with the brightest one in its 5x5 neighborhood. As a result, we obtain a set of brighter edge pixels, which belongs to DW's, and other non-DW edge pixels such as the edges of teeth that may not be as bright in general but enough to pass Canny filter.

Step 2) Intensity thresholding: Remove non-DW edges. We take the intensity histogram of the resulted image from Step 1 and smooth it with moving average filter. As the edges of DW's have higher intensity than those non-DW's, we take the right most valley of the histogram as the intensity threshold and filter the image with this threshold. As a result, most of the non-DW edges are filtered out except few that are as bright as DW edges due to uneven illumination of the radiograph. Nevertheless, these remained non-DW edges are not as connected as DW edges, according to our observation.

Step 3) Contour-length thresholding : Remove the remaining non-DW edges. We compute the length of each connected contour and filter out the ones with length < the preset threshold, which is set by trail and error. At this time, the extracted contours of DW's may not be all complete, as shown in circle in Figs. 2(c) and (d), where (a) and (b) are the original images.

Stage 2: Obtain complete DW's by region growing. We use the center point of each located contour as the seed and grow outward from it to obtain a complete DW [8]. Figs. 2 (e) and (f) are the well grown DW's from the result of Stage 1.

B. Comparison

We claim that our dental work extraction method can extract DW's in Stage 1 more correctly both in shape and number than methods which threshold the entire image with the right most valley of the intensity histogram without preprocessing. Since dental radiographs often have uneven illumination problem that causes non-DW's such as enamels appeared as bright as or even brighter than DW's, sometimes. Thus, segmenting the entire image using single threshold without preprocessing would often mistake some

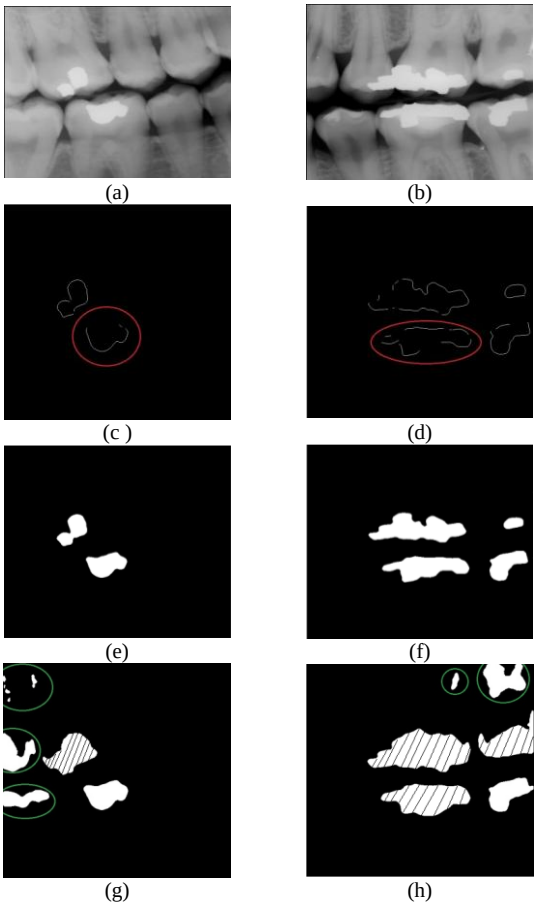

(a) (b) (c) (d) (e) (f) (g) (h)

Figure 2. Detected dental works using our method and Hofer's method. (a),(b): Original radiographs. (c),(d): The stage-1 result of our method. (e),(f):The stage-2 result of our method. (g),(h): The Stage 1 result of Hofer's method.

non-DW's as DW's. Fig. 2 gives two such examples. Notice that the left half of the image in (a) is indeed brighter than the right half and that the right half of the image in (b) is brighter than the left half, thus non-DW's, as shown in the circled regions in (g) and (h), are falsely extracted when both images are segmented by global thresholding [7]. Notice also that the shapes of some DW's segmented this way are somewhat distorted, as shown in the shaded regions in (g) and (h).

III. MATCHING DENTAL WORKS

Shape and size are two common features used in most matching processes. d_{dw} is the metric used in [3] to measure the shape difference of DW's in a pair of neighboring teeth using the minimum of the misaligned region between DW_{PM} and DW_{AM}, where DW_{PM} and DW_{AM} are the DW in PM tooth and AM tooth, respectively. Since the query DW_{PM} must be affine transformed against each DW_{AM} for computing the size of the misaligned region, the difference between these two DW's in translation, rotation, and scale will all be neglected. However, two DW's with the same shape but different orientation/position should be considered from two different subjects, as shown in Figs. 3(a) and (c). If any imposter DW (e.g., Fig. 3(c)) is very similar to the genuine DW (e.g., Fig. 3(a)) but is in different orientation/position/size, the d_{dw} of the imposter DW could be smaller than that of the genuine DW (e.g., Fig. 3(b)), which will lead to a matching error. Figs. 3(d) and (e) illustrate such problem. Notice that d_{dw} in (e) (almost =0) is much smaller than d_{dw} in (d).

In order to include spatial information besides shape among the matching criteria while tolerating the differences caused from imperfect alignment and boundary disturbances, we propose using a spatial domain feature and a frequency domain feature.

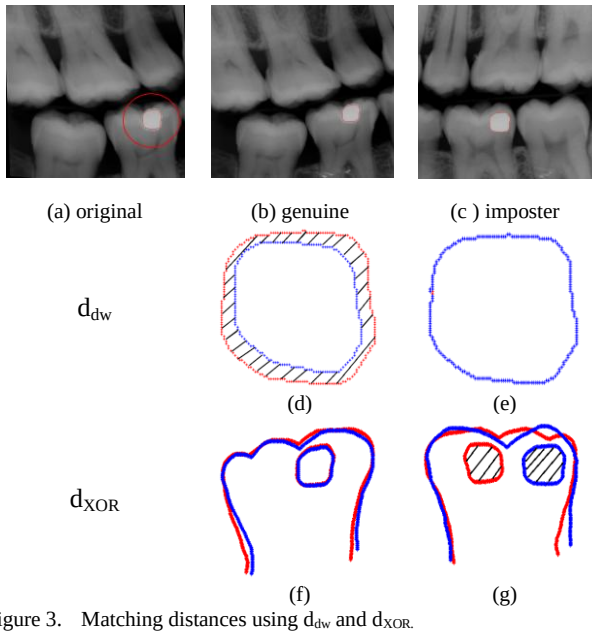

Figure 3. Matching distances using d_{dw} and d_{XOR}.

A. d_{XOR}

d_{XOR} is a spatial domain feature that measures the relative size of the misaligned region between the DW_{PM} and the DW_{AM} against which the DW_{PM} is affine transformed with the optimum parameters obtained from the best tooth contour matching. When two completely identical DW's are perfectly aligned, the size of two DW's under "exclusive or" operation should be 0. Thus, the smaller the size is, the better the two matches. d_{XOR} can be computed using

$$d_{XOR} = \frac{\left|(DW_{PM} \oplus DW_{AM})\right|}{\left|DW_{PM}\right| + \left|DW_{AM}\right|} \quad (1)$$

,where $\oplus$ is the exclusive OR operator, and $|x|$ stands for the size of x. Figs. 3(f) and (g) show the respective d_{xor}'s (in shade) between Figs. (a) (b) and (a) (c), respectively. We can see that d_{xor}(a, b) (almost =0) is smaller than d_{xor}(a, c).

However, d_{xor} creates another problem when the alignment on tooth contours is not perfect and the shapes of their respective DWs are similar. Fig. 4 illustrates such an example, where (a) is a PM tooth, (b) is a genuine AM tooth, (c) is an imposter AM tooth, and (d), (e) are (a) aligned against (b), (c), respectively. Notice that the contour alignment in (e) appears better than that in (d), and that the area of the XORed result in (e) also appears smaller than that in (d). For eliminating the errors resulted from imperfect alignment between tooth contours, we propose another metric d_{FD} as described in follows.

B. d_{FD}

d_{FD} is a frequency domain metric that measures the difference between two sets of Fourier descriptors (FD) that has useful properties including simplicity of implementation and concentration of the contour information in the first few coefficients. In general, the top 10~20% of the descriptors are enough for differentiating two different shapes [8],[10]. Although d_{FD} achieves the same objective as d_{dw}, it is not as

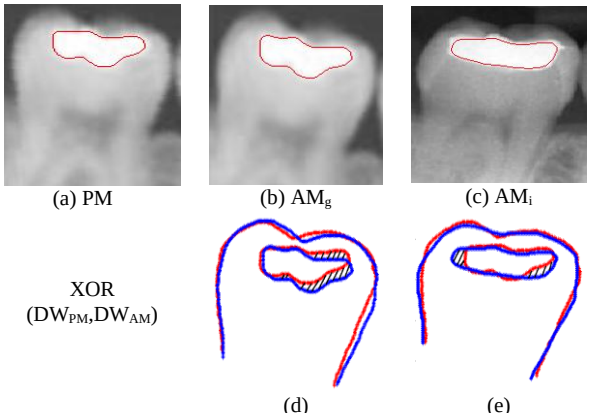

d_{XOR}	0.2370	0.1535
d_{FD}	0.0130	0.0517

Figure 4. An example showing that using d_{FD} can compensate matching errors made by d_{XOR}.

sensitive to boundary disturbances and is more efficient in computation time, as no alignment between the objects are required.

The contour of the DW is represented as a series of N complex numbers $u(n)= x(n)+jy(n)$, $n=1,\ldots,N$, and these N complex numbers are Fourier transformed. The resulted series of coefficients is then normalized using

$$f = \left[\frac{|U(2)|}{|U(1)|}, \frac{|U(3)|}{|U(1)|}, \ldots, \frac{|U(N-1)|}{|U(1)|} \right] \quad (2)$$

, where

$$U(s) = \frac{1}{N} \sum_{n=0}^{N-1} u(n) \mathrm{e}^{-j(2\pi sn/N)} \quad (3)$$

, $s = 0,1,\ldots,N-1$, is the s^{th} Fourier transform coefficient.

Notice that discarding the first coefficient in (3) is to achieve translation invariance, dividing all other coefficients by the second coefficient is to achieve scale invariance, and taking the magnitude of the coefficients is for rotation invariance [11].

d_{FD} can be computed as the root mean square error (RMSE) of the two sets of FD using

$$d_{FD} = \left(\frac{1}{nc} \sum_{k=1}^{nc} \left| F_1^k - F_2^k \right|^2 \right)^{\frac{1}{2}} \quad (4)$$

, where F_1^k, F_2^k are the k^{th} normalized FD of set 1 and set 2 obtained from (2), (3) and nc is the total number of FDs used for each set.

For the radiographs shown in Figs. 4 (a)-(c), both d_{FD} and d_{XOR} of (a, b) and (a, c) are (0.2370, 0.1535) and (0.0130, 0.0517), respectively, which show that matching with d_{FD} can indeed compensate matching errors of d_{XOR} caused from imperfect alignment.

IV. Experiment Results and Analysis

We create a database of 54 AM and 11 PM images. Most of the PM images are in fact the radiographs of our team members, and they are affine transformed or slightly modified to emulate the corresponding AM images. The other AM images used as the hoax identities are collected from Google Images [12]. Since we are only interested in those images having DW(s), thus we use ten PM images containing a total of 21 DW's to query 25 AM images containing a total of 52 different shaped DW's in the first experiment. In the second experiment, 29 AM images containing a total of 57 DW's in which some are hoax DW's (i.e., they have the same shape as some genuine DW's but different orientation/position) are tested. Fig. 5 shows some PM and AM images used in our experiments. In each experiment, matching based on d_{FD} is conducted first followed by matching based on d_{XOR}.

For each DW_{PM}, we directly compute d_{FD} of each test DW_{AM} and rank all d_{FD}'s in an ascending order. Finally we set the rank of each DW_{AM} as its similarity score. For d_{XOR}, we first superimpose the extracted DW image onto the original image so that each DW is located within the correct tooth. Each PM tooth that contains the query DW is then aligned against the AM tooth using the best matching distance computed by the method in [6]. The query DW_{PM} is then affine-transformed using the optimum affine parameters obtaining from the best matching so that two DW's under matching will be well aligned. Finally, XOR of the two DW's is performed. All d_{XOR}'s are then ranked in an ascending order and the rank of each DW_{AM} is set as its similarity score.

Table I shows the comparison of retrieval accuracy of the experiment 1. Among all 21 queries from a total of 52 different shaped DW_{AM}'s, the accuracy of d_{FD} is 16/21(=76%) using the top-1 retrieval; whereas the accuracy of d_{XOR} is 14/21(=67%). The accuracy of d_{FD} increases to 81% if the top 30% of FDs are used. Using top-2 retrievals, d_{FD} recalls four genuine DW's and d_{XOR} recalls three. The accuracy of d_{FD} reaches to 100% using top-8 retrievals;

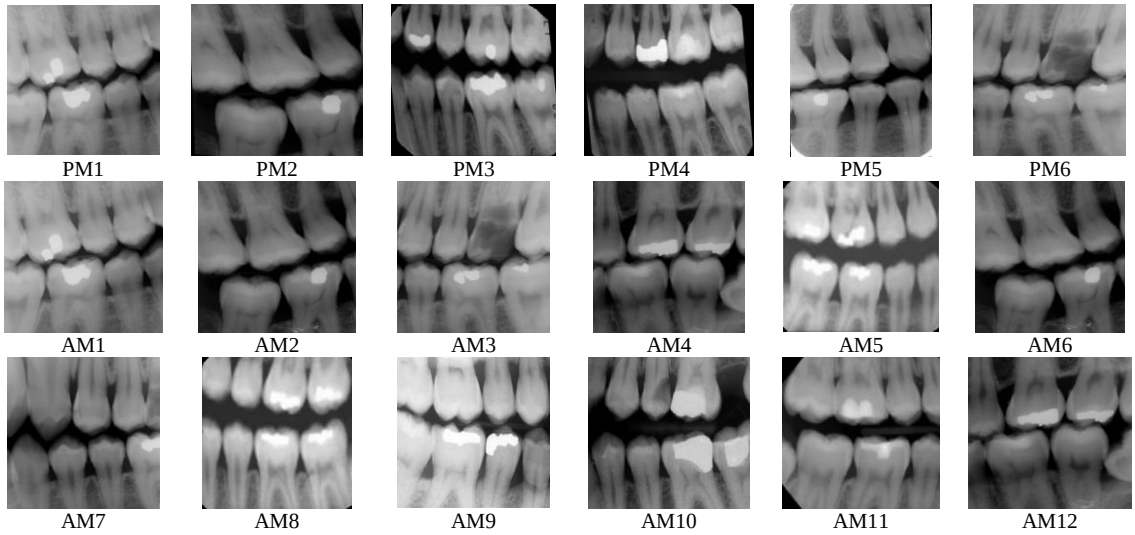

Figure 5. Some PM and AM images used in the experiments.

TABLE I. COMPARISON ON RETRIEVAL ACCURACY OF THE DATABASE WITHOUT HOAX DW'S

Top	2%	4%	6%	10%	17%	44%
Top-	1	2	3	5	8	23
d_{FD}	16/21	20/21	20/21	20/21	21/21	21/21
	76/81*%	95%	95%	95%	100%	100%
d_{XOR}	14/21	17/21	18/21	20/21	20/21	21/21
	67%	81%	86%	95%	95%	100%

Note: the x* is the rate using top30% of FDs.

TABLE II. COMPARISON ON RETRIEVAL ACCURACY OF THE DATABASE WITH HOAX DW'S

Top	2%	4%	5%	9%	16%	47%
Top-	1	2	3	5	9	27
d_{FD}	13/21	19/21	20/21	20/21	21/21	21/21
	62/67*%	90%	95%	95%	100%	100%
d_{XOR}	14/21	17/21	18/21	20/21	20/21	21/21
	67%	81%	86%	95%	95%	100%

Note: the x* is the rate using top30% FDs.

whereas d_{XOR} recalls one each at top-3, -5 and reaches to 100% at top-23 retrievals.

Table II shows the comparison of retrieval accuracy of the experiment 2. Among all 21 queries from a total of 57 DW_{AM}'s in which some are hoax DW's, the accuracy of d_{FD} drops to 13/21(=62%) using the top-1 retrieval; whereas the accuracy of d_{XOR} remains the same. d_{FD} recalls six and one genuine DW's using top-2 and -3 retrievals, and reaches to 100% using top-9 retrievals; whereas d_{XOR} recalls three, one, and two genuine ones using top-2, -3, and -5 retrievals, and reaches to 100% at top-27 retrievals. Comparing with the 95% and 100% hit rates using respective top 8% and 47% retrievals based on a combined metric d_{dw}, which was reported in [3], the metric d_{FD} not only is more efficient but gives a better result.

Meanwhile, comparing the data in both tables, we found that the retrieval using d_{FD} missed three more matches in the experiment 2 than in the experiment 1 when using the top-1 retrieval; whereas using d_{XOR} did not miss any one more. As mentioned earlier, the database for the experiment 2 contains five hoax DW's, which are similar to some genuine DW's in shape but different in orientation/position. Thus, this result shows again that using d_{FD} as the only metric will indeed confuse retrievals from a set of dental works having similar shape but different position/orientation. However, that using d_{XOR} was not affected by hoax DW's suggests that both d_{FD} and d_{XOR} can compensate the drawback of each other when matching the DW_{PM} with hoax dental works.

V. CONCLUSION

We presented a dental work extraction and matching method for bitewing radiographs. Our method includes an algorithm that can correctly extract DW's from radiograph images and two matching metrics d_{FD} and d_{XOR} that can effectively match a postmortem DW to the genuine antemortem DW in the database. The experimental results show that our DW extraction method can extract DW's more correctly than methods using global thresholding. The results also show that, for a database with or without hoax DW's, both metrics achieve about 95% accuracy when using top 6% and 10% retrievals, respectively. The results also indicate that d_{FD} and d_{XOR} can compensate each other when matching a postmortem DW against hoax DW's. Comparing with the 95% and 100% hit rates using top 8% and 47% retrievals from a much bigger database reported in literature, the metric d_{FD} not only is more efficient but gives a better result. Our future works include enhancing the extraction algorithm for images of poor quality and a method of fusion both metrics as well as retrieval with multiple dental works so that a better hit rate based on the top-1 retrieval can be achieved.

ACKNOWLEDGMENTS

This research was supported by the National Science Council of ROC under grant # NSC 98-2221-E-126-009.

REFERENCES

[1] P.L. Lin, Y.H. Yan, P.W. Huang, "An effective classification and numbering system for dental bitewing radiographs using teeth region and contour information," Pattern Recognition, Vol. 43, No. 4, pp. 1380-1392, 2010.

[2] Anil K. Jain and Hong Chen, "Matching of dental X-ray images for human identification," Pattern Recognition, Vol.37, pp. 1519-1532, 2004.

[3] H. Chen and A.K. Jain, "Dental Biometrics: Alignment and Matching of Dental Radiographs," IEEE Transactions on Pattern Analysis and Machine Intelligence, Vol. 27, pp. 1319-1326, 2005.

[4] J. Zhou and M. Abdel-Mottaleb, "A Content-based System for Human Identification based on Bitewing Dental X-ray Images," Pattern Recognition, Vol. 38, pp. 2132-2142, 2005.

[5] O. Nomir and M. Abdel-Mottaleb, "A System for Human Identification from X-ray Dental Radiographs," Pattern Recognition, Vol. 38, pp. 1295-1305, 2005.

[6] J. Ho, A. Peter, A. Ranganranjan, M. Yang, "An Algebraic Approach to Affine Registration of Point Sets", ICCV, 2009.

[7] M. Hofer and A.N. Marana, "Dental Biometrics: Human Identification Based on Dental Work Information," XX Brazilian Symposium on Computer Graphics and Image Processing, pp. 281-286, 2007.

[8] R. Gonzalez and R. Wood, Digital Image Processing 2/e, Prentice Hall, 2002.

[9] J.F Canny, "A Computational Approach to Edge Detection," IEEE Transactions on Pattern Analysis and Machine Intelligence, Vol. 8, pp. 679-698, 1986.

[10] A. McAndrew, An Introduction to Digital Image Processing With Matlab 1/e, Course Technology, 2004.

[11] M. Mahoor and M. Abdel-Mottaleb, "Classification and numbering of teeth in dental bitewing images," Pattern Recognit., vol. 38, pp.577–586, Apr. 2005.

[12] http://www.google.com/imghp